Ecological Indicators 176 (2025) 113643

Contents lists available at ScienceDirect

Ecological Indicators

journal homepage: www.elsevier.com/locate/ecolind

Original Articles

Response and resilience of farmland ecosystems to flash drought in China

Yuanxin Dai [a], Mengyuan Xu [b], Jinlong Dong [a], Ning Yao [a,*], Yi Li [a,*], Shibin Liu [c], Tehseen Javed [d], La Zhuo [e], Qiang Yu [e]

[a] College of Water Resources and Architectural Engineering/Key Lab of Agricultural Water and Soil Engineering of Education Ministry, Northwest A&F University, Yangling, Shaanxi 712100, China
[b] Institute of Agricultural Science and Technology Information, Shanghai Academy of Agricultural Sciences, Shanghai 201403, China
[c] College of Ecology and Environment, Chengdu University of Technology, 1# Dongsanlu, Erxianqiao, Chengdu 610059 Sichuan, China
[d] Department of Environmental Sciences, Kohat University of Science and Technology, Kohat 26000, Pakistan
[e] Institute of Soil and Water Conservation, Northwest A&F University, Yangling, Shaanxi 712100, China

ARTICLE INFO

Keywords:
Flash droughts
Heat wave flash drought
Precipitation deficit flash drought
Farmland ecosystems
Net primary productivity
Drought resilience

ABSTRACT

Flash droughts negatively impact agricultural ecosystems and threaten food security due to their rapid development and unpredictability. This study utilized reanalyzed data from 2000 to 2018 and employed a comprehensive index method to identify two flash droughts: heat wave flash droughts (HWFD) and precipitation deficit flash droughts (PDFD). We analyzed the spatiotemporal evolution of these droughts across China's farmland ecosystems and investigated the response patterns of these ecosystems to both types of flash droughts using response frequency and response time metrics. Our findings indicate that between 2000 and 2018, flash droughts were most frequent in June, with the highest frequency and most extended duration occurring in summer and the lowest in autumn. Spatially, HWFD frequency was highest in the Loess Plateau, with durations of 4.4 and 5.0 octads, while PDFD was most frequent in the Gansu-Xinjiang (GX) and Huang-Huai-Hai (HHH) regions. Over time, there was a decrease in the frequency and duration of flash droughts. The study revealed that Net Primary Productivity (NPP) generally exhibited a low response frequency to flash droughts, with PDFD showing a higher response frequency and a shorter response time than HWFD. Irrigated farmland showed higher NPP response frequencies, particularly in the HHH region, whereas rainfed farmland demonstrated stronger resilience to flash droughts. This research provides theoretical support for developing flash drought early warning systems and drought mitigation policies, significantly contributing to food security in China's farmland ecosystems.

1. Introduction

Flash drought is a typical drought event that occurs suddenly and intensifies rapidly due to high temperatures and below-normal precipitation. It is often accompanied by a sharp decline in soil moisture, which can lead to severe agricultural losses because of the lack of early warnings (Tyagi et al., 2022; Gerken et al., 2018; Liu et al., 2020; Yuan et al., 2018). For example, the severe flash drought in the United States in 2012 induced the drop of corn yield to the lowest level since 1995, resulting in direct economic losses amounting to hundreds of billions of dollars (Otkin et al., 2016). China has also experienced many flash drought events in recent years (Yuan et al., 2015; Ren et al., 2023). In the context of global warming, flash droughts are expected to occur more frequently (Yuan et al., 2023; Mahto and Mishra, 2023). Therefore, studying the changes in flash droughts in farmland is important for agricultural management and food security.

The indices used to define and quantify flash droughts must reflect the short-term variability of the variables involved. Currently, there are three main methods for identifying flash droughts. The first method is the integrated index approach, which involves using multiple indicators

Abbreviations: HWFD, heat wave flash droughts; PDFD, precipitation deficit flash droughts; HWFD-I, HWFD in irrigated cropland; HWFD-R, HWFD in rain-fed cropland; PDFD-I, PDFD in irrigated cropland; PDFD-R, PDFD in rain-fed cropland; QT, Qinghai-Tibet; S, South China; SW, Southwest; YRML, the Middle and Lower reaches of the Yangtze River; IMGW, Inner Mongolia and along the Great Wall; NE, Northeast; LP, Loess Plateau; HHH, Huang-Huai-Hai; GX, Gansu-Xinjiang; NPP, Net Primary Productivity; SESR, Standardized Evaporative Stress Ratio; GLDAS, Global Land Data Assimilation System; SM, Soil Moisture; GPP, Gross Primary Productivity.

* Corresponding authors.
E-mail addresses: yaoning@nwafu.edu.cn (N. Yao), liyi@nwafu.edu.cn (Y. Li).

https://doi.org/10.1016/j.ecolind.2025.113643
Received 9 December 2024; Received in revised form 7 May 2025; Accepted 20 May 2025

to identify flash droughts based on their values over a specific period. Mo and Lettenmaier (2015, 2016) proposed the uses of temperature, evapotranspiration, and soil moisture on a pentad scale to identify heat wave flash droughts (HWFD) and precipitation deficit flash droughts (PDFD) together. The second method emphasizes the development rate of flash droughts. Ford and Labosier (2017) used the percentile of soil moisture averaged over pentad and the rate of decline in soil moisture to identify flash droughts. Christian et al. (2021) used Standardized Evaporative Stress Ratio (SESR) and identified flash droughts based on changes in SESR over time. The third approach identifies flash droughts by considering multiple processes involved in flash droughts, along with their development rates. Yuan et al. (2019) used soil moisture percentile to identify flash droughts, considering different processes and the persistence of flash droughts. The criteria for identifying flash droughts included a rapid decline in average soil moisture percentile from 40 % to 20 %, with a decline rate exceeding 5 % and lasting at least 15 days. The flash drought was terminated when the soil moisture percentage recovered above 20 %. The latter two approaches highlight a crucial distinction between flash and traditional droughts: their rapid development. They classify flash droughts as a type of drought defined by a certain level of persistent water shortage. However, relying on a single variable or indicator simplifies the classification of flash drought events, as no single indicator can capture the complex processes and diverse impacts of flash droughts. Therefore, this study used the method proposed by Mo and Lettenmaier (2015, 2016) to identify flash droughts, which considers multiple variables and different causes of flash droughts.

The farmland ecosystem is a major subsystem of the broader agricultural system and an essential component of terrestrial ecosystems. It is a semi-natural ecosystem for human utilization of natural resources and the production of agricultural activities. Globally, cropland accounts for 38 % of the land area and provides 66 % of the world's food supply. Farmland ecosystems support agricultural productivity, ensure food security, regulate carbon cycling, and influence global climate change. With global warming, increasing intensity and frequency of flash droughts pose significant threats to these ecosystems. Given these threats, flash droughts, driven by moisture deficiency, can directly slow down or halt crop growth, thereby threatening agricultural output. Additionally, flash droughts can indirectly impact crop health and farmland stability by elevating the risks of wildfires, pest outbreaks, and disease spread. These combined effects highlight the vulnerability of farmland ecosystems to flash droughts in a warming climate (Griffin-Nolan et al., 2019).

Flash droughts' impact on agriculture primarily manifests through two pathways: direct physiological stress and indirect ecological risks. Regarding direct physiological stress, water deficits directly inhibit photosynthesis and plant cell division, leading to stunted growth or even death (Otkin et al., 2018). At the same time, the combined effects of high temperatures and high evaporation rates accelerate the depletion of soil moisture, creating a positive feedback loop of "soil–vegetation" water stress. Regarding indirect ecological risks, vegetation wilting caused by flash droughts increases the accumulation of surface combustible materials, raising the probability of wildfires. These secondary disasters directly destroy crops and weaken the ecosystem's carbon sink function by releasing CO_2 through the combustion of organic matter.

These impacts have been confirmed in studies from various regions around the world. For example, the flash drought in the US Midwest in 2012 significantly reduced vegetation growth and carbon uptake, with Gross Primary Productivity (GPP) in corn, soybeans, croplands, and grasslands decreasing by 9 %, 7 %, 6 %, and 29 %, respectively (Jin et al., 2019). Similarly, flash droughts in Europe have negatively impacted vegetation conditions and carbon absorption (Sungmin and Park, 2023). More severe flash droughts in western and southwestern Central Asia led to decreased GPP, and agricultural areas showed heightened sensitivity to these changes (Zhu et al., 2025). Moreover, vegetation with shallow roots, such as cropland and grassland, responds more rapidly to flash droughts (Lu et al., 2024). During flash droughts, the average Net Primary Productivity (NPP) loss rate exceeds 60 %, and the minimum daily economic loss is over 12 million yuan in the Xilingole Grassland (Liu et al., 2024). Compared with slowly developing droughts, flash droughts during the growing season pose higher ecological risks, with ecosystem productivity experiencing faster decline rates and shorter response times (Zhang et al., 2025).

Globally, the impact of flash droughts on agricultural yields is particularly significant. In South America, flash droughts significantly reduce crop yields. In the central, southeastern regions, flash droughts from November to January disrupt crops' flowering and grain-filling stages. In the northern southeastern areas, flash droughts from February to April mainly affect second-season corn, leading to substantial yield losses (Lovino et al., 2025). In late July 2019, a severe flash drought occurred in the southern agricultural zones of China, leading to a rapid depletion of soil moisture. This caused a sharp decline in the photosynthetic capacity of crops in the affected areas and a significant reduction in food production (Zhang et al., 2024). In 2010, a flash drought in western Russia, which began in June and intensified rapidly, severely impacted the agricultural ecosystem. By early July, nearly all major wheat-producing regions were affected by extreme water stress, coinciding with the flowering stage of both winter and spring wheat. This led to a drastic reduction in wheat yields—over 70 % in top-producing areas—and a total production loss of 20 million metric tons compared to previous seasons (Hunt et al., 2021). These cases demonstrate that the impact of flash droughts on agricultural ecosystems is far-reaching and multifaceted, directly reducing crop yields and weakening ecosystems' stability and carbon sink capacity through various pathways.

To better understand these impacts, many studies have utilized indicators such as GPP, NPP, Leaf Area Index (LAI), Water Use Efficiency (WUE), Solar-Induced Fluorescence (SIF), Mean Annual Precipitation (MAP), and vegetation indices to evaluate the impact of flash droughts on agricultural ecosystems through response frequency and response time (Poonia et al., 2022; Sungmin and Park, 2023; Yang et al., 2023; Yao et al., 2022; Zhang et al., 2020; Zhao et al., 2024).However, many of these studies consider farmlands uniform systems, while human management significantly influences field interactions (Zhu et al., 2021). Irrigation is a common management practice to cope with extreme weather events such as droughts in farmlands (Troy et al., 2015; Jiang et al., 2019). Only 20 % of agricultural land worldwide is irrigated, yet it accounts for 40 % of global agricultural output, which means that irrigation more than doubles land productivity (FAO, 2003). Therefore, understanding the impact of flash droughts on farmland ecosystems requires examining the different responses of irrigated and rain-fed farmlands. Additionally, the timing and sensitivity of flash drought impacts on vegetation vary depending on the drought stage and the specific region (Liu et al., 2024). For instance, Xu et al. (2021) showed that vegetation photosynthesis responded to drought quicker and stronger with increasing dryness.

Here, we employed a comprehensive indicator approach to identify flash droughts and used response frequency and time to deeply examine the response processes of rain-fed and irrigated farmland ecosystems in different regions. The main research objectives were (1) to analyze the spatial and temporal evolution of flash droughts and their trend patterns in China's farmland from 2000 to 2018; (2) to explore the response of different regional farmland ecosystems to flash droughts under different management measures (irrigation and rainfed) using NPP data; and (3) to analyze NPP values at different stages of flash droughts and study the resilience of farmland to flash droughts in different regions. The findings of this study provide theoretical support for the early warning of flash drought in different farmland ecosystems and the formulation of drought mitigation policies in China, which is of great practical significance for food security.

2. Materials and methods

2.1. Study area

The climate in China is complex and varied, with tropical monsoon, subtropical monsoon, temperate monsoon, temperate continental, and high mountain plateau climates distributed from south to north (Xiao et al., 2013). Precipitation decreases gradually from the south-east coast to the north-west interior, with abundant rainfall in summer and scarce rainfall in winter. Temperatures gradually decrease from south to north, with significant regional temperature differences in winter and summer. Based on the principles of agricultural production conditions, characteristics and direction of development, significant problems and key measures, and the completeness of administrative units, the Chinese Committee on Agricultural Zoning divides the country into nine agricultural zones (Fig. 1).

2.2. Data sources

This study utilized the GLDAS-2 assimilation dataset for flash drought identification because of its high reliability and applicability in drought research (Liu et al., 2020). The GLDAS-2.1 (Noah model) data product has a spatial resolution of 0.25° × 0.25° and a temporal resolution of 3-hourly intervals (https://disc.gsfc.nasa.gov/ datasets/GLDAS_NOAH025_3H_2.1/summary). Temperature, evapotranspiration, and soil moisture data for 2000–2018 from this dataset were used. The acquired data were pre-processed by the following steps: First, the 3-hour data were extracted and converted into daily data (averaging the temperature and soil moisture, and summing the evapotranspiration). In addition, the ET and the soil moisture data require unit conversion. To convert the units of ET from kg m^{-2} s^{-1} to mm h^{-1}, dividing the density (1000 kg m-3) by multiplying time (3600 s) is necessary. Soil moisture data must also be converted from kg m^{-2} to m^3 m^{-3}. The conversion formula is as follows:

$$\theta = \frac{w}{\rho \times h} \times 100\% \tag{1}$$

where θ is the volumetric soil water content (m^3 m^{-3}); w is the GLDAS soil moisture (kg m^{-2}); ρ is the density of water (kg m^{-3}), ρ = 1000 kg m^{-3}; h is the soil layer thickness (m).This study used GLDAS soil moisture at depths of 0–10 cm, 10–40 cm, and 40–100 cm, so h is 0.1 m or 0.3 m or 0.6 m. Finally, the soil moisture data from 0-10 cm, 10–40 cm, and 40–100 cm were converted to 0–100 cm by multiplying and summing the corresponding weights (0.1, 0.3, and 0.6, respectively).

Net Primary Production (NPP) (g C m^{-2} d) is the net carbon flow entering plants from the atmosphere, representing the remaining organic matter after subtracting the autotrophic respiration losses from Gross Primary Productivity (GPP). The NPP data for the years 2000–2018 was obtained from the MUSES 5-km global GPP and NPP products dataset (Sun et al., 2020). The product estimates GPP and NPP using Light Use Efficiency (LUE) and a long-term series of Global Land and Landsat (GLASS) LAI and Fraction of Photosynthetically Active Radiation (FPAR) from 1981 to 2018. The product has a temporal resolution of 8 days and a spatial resolution of 0.05°×0.05°. In this study, the data was resampled to 0.25°×0.25° in R Studio to standardize the resolution.

Land use data were obtained using the European Space Agency (ESA) Climate Change Initiative Land Cover (v2.0.7 and v2.1.1) (https://cds.climate.copernicus.eu/ datasets/satellite-land-cover?tab = overview). This dataset provides a global map of land use and contains 22 land use categories. The long-term consistency, annual updating, and high resolution of the dataset on a global scale make it attractive for many fields (Defourny et al., 2017). The temporal resolution of this dataset is annual, and the spatial resolution is 300 m. In this study, the data was resampled to 0.25°×0.25° in RStudio to standardize the resolution. Then, the grids for irrigated and rainfed farmland for nineteen consecutive years were extracted based on attributes 10 and 20 (Table S1 and Fig. S1). Due to the limited number of grid points in QT and IMGW, these areas are not considered in the comparison.

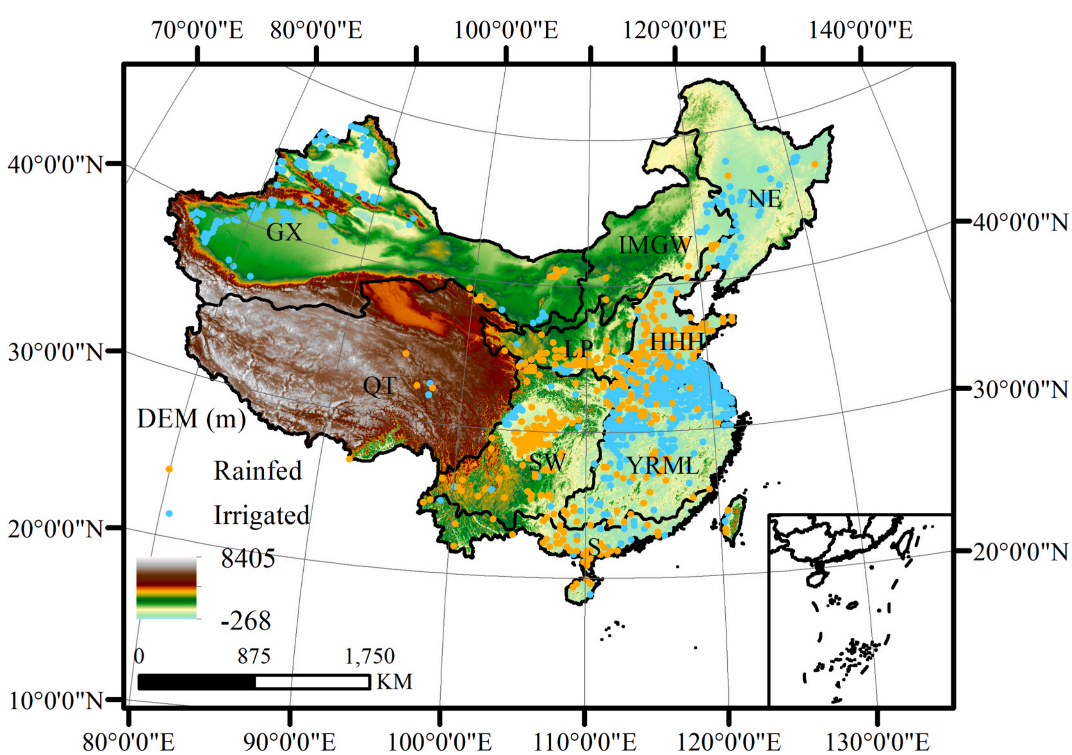

Fig. 1. Agricultural zoning and Digital Elevation Model (DEM) map of China. QT, Qinghai-Tibet; S, South China; SW, Southwest; YRML, the Middle and Lower reaches of the Yangtze River; IMGW, Inner Mongolia and along the Great Wall; NE, Northeast; LP, Loess Plateau; HHH, Huang-Huai-Hai; GX, Gansu-Xinjiang.

2.3. Methodology

2.3.1. Identification of flash droughts

This study utilized the method defined by Mo and Lettenmaier (2015, 2016) to identify two types of flash droughts: HWFD and PDFD. HWFD is essentially an agricultural drought. Therefore, soil moisture is used (expressed as a percentile relative to its long-term record, SM%) as an indicator rather than precipitation. Since HWFD is driven by temperature, the temperature anomaly must exceed one standard deviation. Additionally, high temperatures increase total evapotranspiration, so the evapotranspiration anomaly must be positive. Furthermore, considering the nature of HWFD, the SM% should be below 40 % (Mo and Lettenmaier, 2015).

PDFD is an event-driven by a lack of precipitation. The reduced rainfall before the event leads to decreases in SM and ET, which causes an increase in temperature. PDFD is also characterized by a deficiency in SM, resulting in crop damage. In this sense, PDFD can also be considered an agricultural drought (Mo and Lettenmaier, 2016). Therefore, to identify PDFD, the temperature anomaly must be positive, the SM% must be below 40 %, and the evapotranspiration anomaly must be negative. We considered vegetation's boundary effects and growth cycles, opting for an 8-day interval to capture multiple stages of the vegetation growth cycle and provide a more averaged representation of vegetation conditions in this study. The definition we are employing here is based on percentile values of soil moisture, temperature anomalies, and total evapotranspiration anomalies (Zhang et al., 2022):

$$\begin{array}{l} HWFD: T_{anomaly} > T_{std}; TET_{anomaly} > 0; \quad SM < 40\% \\ PDFD: T_{anomaly} > T_{std}; TET_{anomaly} < 0; \quad SM < 40\% \end{array} \tag{2}$$

where $T_{anomaly}$ (K) and $TET_{anomaly}$ (mm/day) denote the 8-day mean temperature and total evapotranspiration anomaly, respectively. T_{std} is the standard deviation of the $T_{anomaly}$ series. For each 8 days and each grid point, a flash drought was considered to have occurred at that grid point for this period when all the above requirements were met. The anomaly series was obtained by subtracting the mean of the variables from the observed values.

2.3.2. The frequency of flash drought occurrences

The Frequency of Occurrence (FOC) was calculated to determine the hotspots of flash drought occurrences. For a given 8-day period T and grid point x, when the specified criteria for flash drought are met, we consider the grid point to have experienced a flash drought event. This time is defined as the onset of the flash drought. When the conditions for a flash drought are no longer met, the drought is considered to have ended. For each grid point, we calculate the number of periods N that meet the criteria for flash drought. FOC is the percentage of periods during which the grid point is in either HWFD or PDFD:

$$FOC = \frac{N}{N_{total}} \times 100\% \tag{3}$$

where N_{total} is the total number of periods in the study period. N is the number of periods that satisfy the definition of flash drought.

2.3.3. Trend test for flash droughts

The Modified Mann-Kendall (MMK) method considers all significant autocorrelations in the time series, so this study used the MMK test to analyze the trend changes of flash drought characteristics (Hamed and Rao, 1998). Under the null hypothesis that the sequence has no trend, the statistic Z follows a standard normal distribution with a mean of 0 and a variance of 1. When $\alpha = 0.05$, $|Z| \geq 1.96$, the sequence has a significant trend change; a positive Z indicates a significant increasing trend, and vice versa. The statistic Z* of the MMK trend test method considers the influence of autocorrelation in the sequence, and the estimation method is as follows:

$$Z^* = \frac{Z}{\sqrt{n^s}} \tag{4}$$

$$n^s = 1 + \frac{2}{n(n-1)(n-2)} \sum_{j=1}^{n-1} (n-j)(n-j-1)(n-j-2) r_j \tag{5}$$

where n^s denotes the correction factor, j denotes the number of lags, and r_j denotes the autocorrelation coefficient of the time series.

2.3.4. Response of farmland ecosystems to flash drought

NPP integrates drought's effects on photosynthesis and respiration (Stocker et al., 2018), so this study considers NPP as an ecological indicator to study the ecosystem's response to flash drought. A negative anomaly in NPP indicates the onset of the ecosystem's response. The standardized anomaly is calculated as follows:

$$NPP_{SA} = \frac{NPP - \mu_{NPP}}{\sigma_{NPP}} \tag{6}$$

where NPP_{SA} is the normalized anomaly of NPP, and σ_{NPP} and μ_{NPP} are the standard deviation and mean of the NPP sequence, respectively.

Response time and frequency were used to clarify the relationship between NPP and flash drought (Niu et al., 2018). Response frequency was obtained for each grid by counting the proportion of flash droughts with negative NPP_{SA} to the total number of flash droughts. A lower response frequency indicates a lower risk for the ecosystem and vice versa. The response time index is the days until the first negative standardized anomaly (NPP_{SA}) occurs during the flash drought event. A shorter response time indicates a quicker threat from flash drought (Yang et al., 2023).

2.3.5. Different stages of flash drought and ecosystem resilience to flash drought

In this paper, we adopted the classification of the stage of flash drought by Liu et al. (2024) and divided the development process of flash drought into three stages: flash drought accumulation stage, flash drought outbreak and persistence stage, and flash drought recovery stage. We calculated the corresponding NPP values of the three stages simultaneously. The accumulation stage is defined as the two octads (octad refers to eight days) before the onset of the flash drought, while the outbreak and persistence stage encompasses the period from the onset to the end of the flash drought. The recovery stage is studied for one octad following the end of the drought. The recovery status of various types of farmlands in different regions can be determined by comparing the NPP values of the accumulation and recovery stages. The closer the NPP value of the recovery stage is to that of the accumulation stage, the better the resilience.

3. Results

3.1. The spatiotemporal evolution pattern of flash drought

The occurrence frequency of flash droughts exhibits fluctuations over time (Fig. 2a). The average frequency of HWFD from 2000 to 2018 was 1.15 % in irrigated farmland and 1.17 % in rain-fed farmland. The average frequency of PDFD was 0.19 % in irrigated farmland and 0.13 % in rain-fed farmland. The frequency of HWFD in irrigated cropland (HWFD-I) reached a maximum of 1.64 % in 2014. The frequency of HWFD in rain-fed cropland (HWFD-R) reached the maximum value of 2.30 % in 2011. The frequency of PDFD in irrigated cropland (PDFD-I) reached the maximum value of 0.62 % in 2014. The frequency of PDFD in rain-fed cropland (PDFD-R) reached the maximum value of 0.50 % in 2014. The frequency of both flash droughts was higher in 2014.

The duration of flash droughts exhibited a relatively small variation from 2000 to 2018. The average duration of HWFD-I was 3.4 octads,

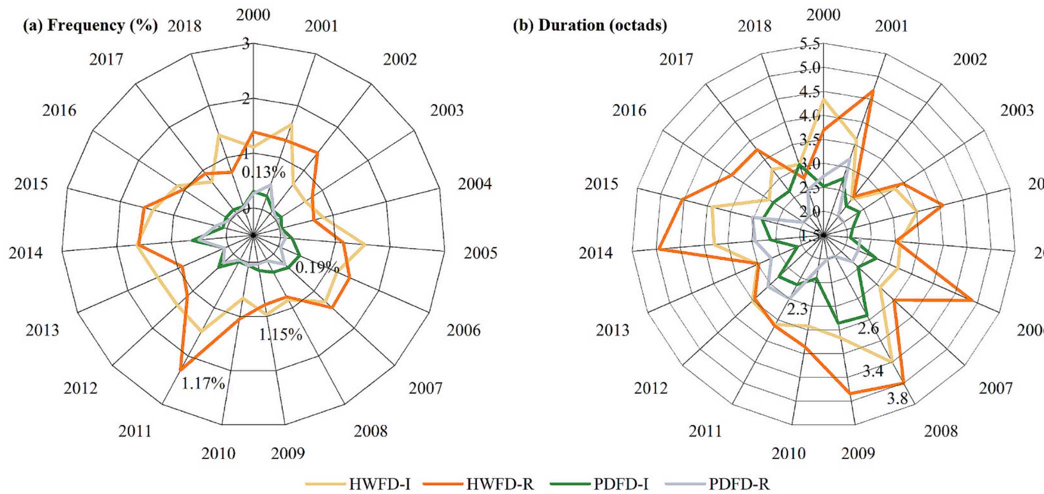

Fig. 2. Annual variation of flash drought properties in different types of farmlands in China from 2000 to 2018. HWFD-I, HWFD in irrigated cropland; HWFD-R, HWFD in rain-fed cropland; PDFD-I, PDFD in irrigated cropland; PDFD-R, PDFD in rain-fed cropland. The values following the lines in the plot represent their corresponding averages.

while the average duration of HWFD-R was 3.8 octads. For PDFD-I, the average duration was 2.6 octads; for PDFD-R, the average duration was 2.3 octads (Fig. 2b). It was observed that the duration of HWFD was longer than that of PDFD. In 2008, the duration was the longest for both HWFD-I and HWFD-R, reaching 4.5 and 5 octads, respectively. For PDFD-I, the most prolonged duration was also in 2008, at 3.4 octads, while for PDFD-R, it was in 2001, at 3.2 octads.

Flash drought occurred mainly from June to August (Fig. 3a). The frequency of occurrence for both types of flash drought was the highest in June and the lowest in autumn. The duration of HWFD was the longest in June, while the duration of PDFD was the longest in May. The duration of both types of flash drought was most extended in summer and shortest in autumn (Fig. 3b).

In general, the occurrence frequency of HWFD exhibits a spatial distribution high in the middle and low at both ends of the farmland (Fig. S2). The main areas with a low occurrence frequency of HWFD were distributed in the S, YRML, and SW (with an occurrence frequency of less than 3.9 %), while the areas with a high occurrence frequency were in LP (with an occurrence frequency greater than 9.62 %). The spatial distribution of the duration of HWFD was similar to that of the occurrence frequency, indicating that once HWFD occurs in these areas, they tend to have a relatively long duration and occur more frequently. Most areas did not experience PDFD, and the areas where PDFD did occur have a relatively low occurrence frequency. The areas with a high occurrence frequency of PDFD were sporadically distributed in the GX (with an occurrence frequency greater than 4.93 %). The duration of PDFD was relatively short in most areas, and the areas with a long duration were mainly distributed in GX. The occurrence frequency of HWFD showed a significant downward trend in 89 % of the grid points, with non-significant downward trends mainly located in the HHH (Fig. S3). The trend distribution of the duration of HWFD was spatially similar to that of the occurrence frequency. The occurrence frequency and duration of PDFD showed a significant downward trend in most areas, with non-significant downward trends at individual points (sporadically distributed in GX). Flash droughts' occurrence frequency and duration have shown a downward trend from 2000 to 2018.

The frequency of HWFD-I was highest in LP at 11.11 %, significantly higher than the 0.67 % observed in S (Fig. 4). A similar pattern was seen for HWFD-R, with LP reporting the highest frequency at 12.97 % and S the lowest at 0.79 %. For PDFD-I, the frequency was notably high in GX at 1.57 %, while it was markedly low in YRML, with only 0.029 % occurrence. In rainfed farmlands, the HHH stood out with the highest frequency of PDFD at 1.17 %, whereas the YRML recorded the lowest at an almost negligible 0.0099 %.

HWFD exhibited their most extended durations in LP for both farmlands, with 4.4 octads in irrigated farmland and 5.0 octads in rainfed farmland. Conversely, the shortest durations were observed in South China, where the figures stood at 2.5 octads for irrigated and 2.7 for rainfed farmland. In the case of PDFD, the most extended durations were found in the SW, amounting to 2.9 octads in irrigated farmlands

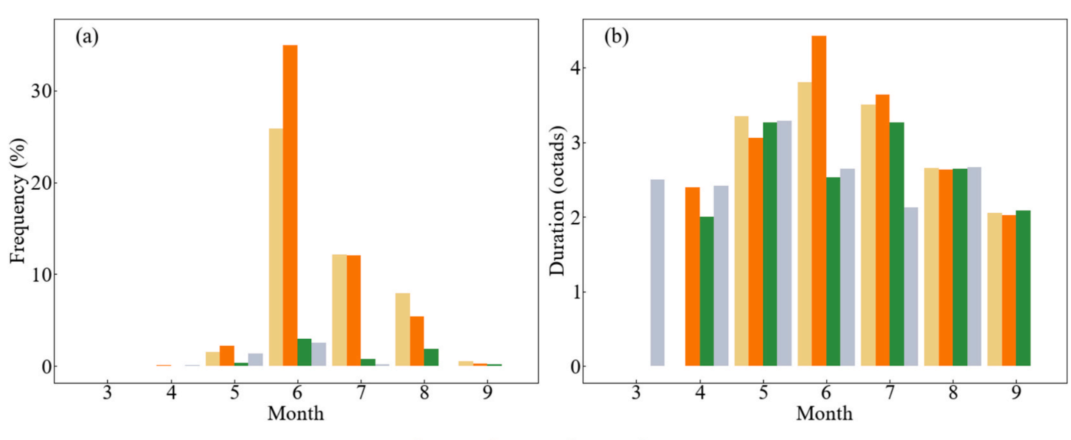

Fig. 3. Monthly variation of flash drought properties in different types of farmlands in China from 2000 to 2018.

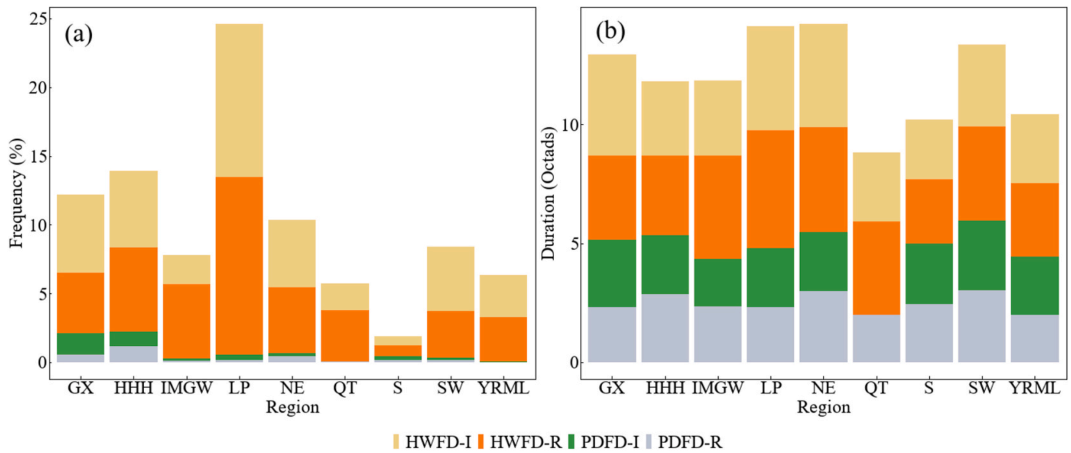

Fig. 4. Percentage of flash drought characteristics in different farmlands in China's agricultural regions from 2000 to 2018. Note: Due to the limited number of grid points in QT and IMGW, these areas are not considered in the comparison.

and 3.0 octads in rainfed farmlands. The shortest durations were recorded in YRML, with 2.4 octads for irrigated farmlands and a minimal 2.0 octads for rainfed farmlands.

The occurrence frequency of HWFD in irrigated and rainfed farmland does not exceed 15 %, with most occurrences concentrated within 0–10 % (Fig. 5). On average, the frequency of HWFD-R (4.55 %) was higher than HWFD-I (3.97 %). The duration of HWFD in irrigated and rainfed farmland typically ranged from 2 to 6 octads. On average, the duration of HWFD-R (3.35 octads) was slightly longer than that of HWFD-I (3.26 octads). Overall, the occurrence frequency of HWFD in rainfed farmland was higher than in irrigated farmland by 0.58 %, and the duration of HWFD in rainfed farmland was more prolonged than in irrigated farmland by 0.09 octads.

The occurrence frequency of PDFD in irrigated and rain-fed farmland was relatively low, primarily concentrated within 0–2 %. On average, the difference between the two was minimal, at 0.51 % for irrigated farmland and 0.36 % for rainfed farmland. The PDFD duration in both farmlands typically spanned from 2 to 5 octads. The duration of PDFD in irrigated farmland (1.2 octads) was slightly longer than that in rainfed farmland (0.9 octad). Overall, the occurrence frequency of PDFD was higher in irrigated farmland than rainfed farmland by 0.16 %, and their duration was also slightly longer in irrigated farmland by 0.3 octad.

3.2. Response of farmland NPP to flash drought

The average response frequency of Net Primary Productivity (NPP) to HWFD from 2000 to 2018 was 22.8 % for irrigated farmland and 15.5 % for rain-fed farmland (Fig. 6). The maximum response frequency of

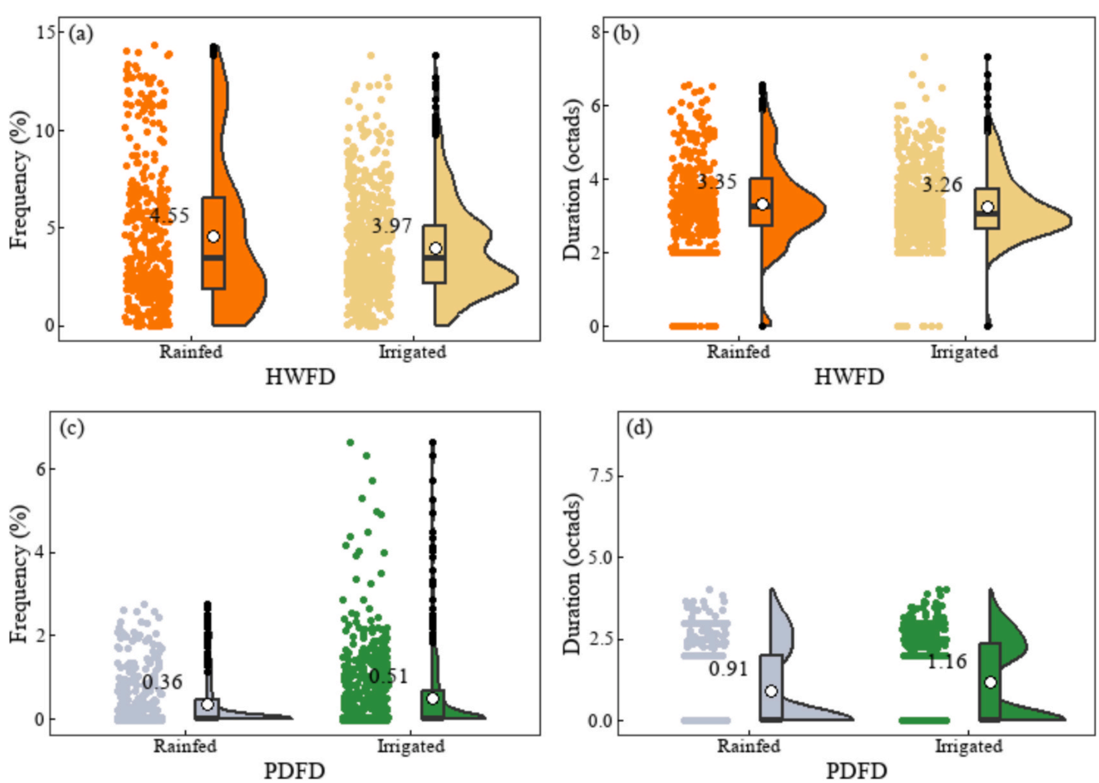

Fig. 5. Distribution pattern of flash drought characteristics in different types of farmlands in China from 2000 to 2018. Notes: The 0 in the figure represents grid points where no flash drought occurs.

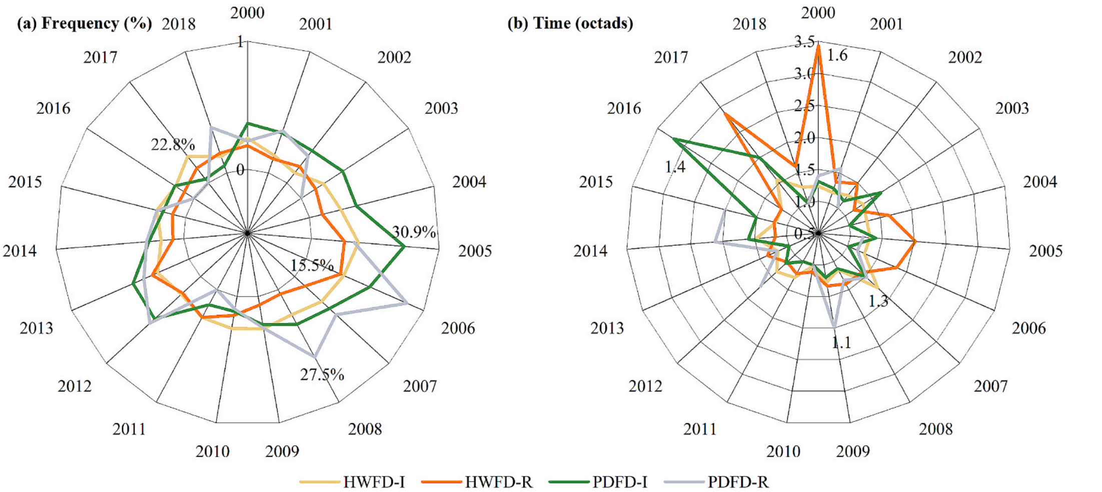

Fig. 6. Annual variation of frequency and time of NPP response to flash droughts in different types of farmlands in China from 2000 to 2018. Notes: The values next to the lines in the plot represent their corresponding averages.

NPP to HWFD reached 36.8 % in 2005 for irrigated farmland and 31.2 % in 2013 for rain-fed farmland. The average response frequency of NPP to PDFD from 2000 to 2018 was 30.9 % for irrigated farmland and 27.5 % for rain-fed farmland. The maximum response frequency of NPP to HWFD was 72.6 % in 2005 for irrigated farmland and 85.7 % in 2013 for rain-fed farmland. Overall, the response frequency of NPP to both types of flash drought was relatively low. By comparing the two types of flash droughts, it was found that NPP has a higher response frequency to PDFD. When comparing the two types of farmland, it was observed that the NPP of irrigated farmland has a higher response frequency to both types of flash droughts. This implies that the NPP of farmland is more sensitive to PDFD, while the NPP of irrigated farmland is sensitive to both types of sudden droughts.

From 2000 to 2018, the average response time of NPP to HWFD was 1.3 octads for irrigated farmland and 1.6 octads for rainfed farmland. The maximum response time of NPP to HWFD was 1.8 octads in 2007 for irrigated farmland and 3.4 octads in 2000 for rainfed farmland. The average response time of NPP to PDFD was 1.4 octads for irrigated farmland and 1.1 octads for rainfed farmland. The maximum response time of NPP to PDFD was 3.2 octads in 2007 for irrigated farmland and 2.1 octads in 2000 for rainfed farmland. By comparing the two types of flash droughts, it can be observed that NPP responds more quickly to PDFD. Additionally, when comparing the two types of farmland, it is found that the NPP of irrigated farmland responds more quickly to both types of flash droughts.

NPP responded to HWFD with an average frequency of 21.2 % in irrigated farmland and 8.8 % in rainfed farmland. Regarding PDFD in the same region, NPP exhibited an average response frequency of 17.3 % for irrigated areas and 8.8 % for those relying on rainfed areas (Fig. S4). In the HHH region, the average response frequency of NPP to HWFD was 26.0 % for irrigated farmland and 17.2 % for rain-fed farmland. For PDFD, the frequencies were notably higher, at 32.2 % for irrigated farmland and 28.6 % for rain-fed farmland. In the IMGW area, the average response frequency of NPP to HWFD was 11.7 % for irrigated farmland and 16.7 % for rain-fed farmland. The response to PDFD was slightly lower, with 10.5 % for irrigated and 5.3 % for rainfed farmland. Within the LP, the average response frequency of NPP to HWFD was 16.0 % for irrigated farmland and 5.8 % for rainfed farmland. The response frequency to PDFD was relatively modest at 5.3 % for irrigated farmlands and 3.4 % for those on rainfed lands. In the NE, average response frequency of NPP to HWFD was relatively low at 4.4 % for irrigated farmland and 12.5 % for rainfed farmland. The response frequency to PDFD was slightly higher, with 5.9 % for irrigated and 2.1 % for rainfed farmland. The QT region exhibited a significant average response frequency of NPP to HWFD, particularly in irrigated farmland at 36.4 % and 14.5 % for rainfed farmland. Interestingly, the response frequency to PDFD was negligible in irrigated areas at 0 %. In comparison, it was 5.3 % in rain-fed farmland. In the South China region, average response frequency of NPP to HWFD was 10.4 % in irrigated farmland, notably higher at 30.2 % in rain-fed farmland. The response to PDFD was also higher, with 17.6 % in irrigated farmland and 25.1 % in rain-fed farmland. In the SW region, average response frequency of NPP to HWFD was 22.1 % in irrigated farmland and 19.2 % in rain-fed farmland, while the response to PDFD was 14.2 % in irrigated and 8.4 % in rain-fed farmland. In the YRML region, average response frequency of NPP to HWFD was 21.4 % in irrigated farmland and 22.4 % in rain-fed farmland. The response frequency to PDFD was relatively low at 9.5 % for irrigated farmland and 0 % for rainfed farmland.

In the GX region, the NPP of farmland responded to HWFD with an average duration of 1.6 octads for irrigated areas and 0.4 octads for rainfed areas. Conversely, the response time to PDFD averaged 1.4 octads for irrigated lands and 0.2 octads for those sustained only by rainfall. Within the HHH region, the average response time of NPP to HWFD was 1.2 octads for irrigated farmland and 1.3 octads for rainfed farmland. For PDFD, the average durations were 0.7 octads for irrigated and 0.8 octads for rainfed farmland. In the IMGW area, the average response time of NPP to HWFD was a brief 0.2 octad for irrigated farmland and 0.3 octad for rainfed farmland. The response time to PDFD was minimal, at 0.1 octads for irrigated and rainfed farmland. On the LP, the average response time of NPP to HWFD was more pronounced at 1.7 octads for irrigated farmland and 1.4 octads for rainfed farmland. The response time to PDFD was slightly lower, with 0.2 octad for irrigated and 0.3 octad for rainfed farmland. In the NE, the average response time of NPP to HWFD was 0.5 octad for irrigated farmland and 0.3 octad for rainfed farmland. The response to PDFD was consistent at 0.1 octads for both types of farmland. The QT region, exhibited a moderate average response time of the NPP to HWFD, with 0.5 octad for irrigated farmland and 0.9 octad for rainfed farmland. The response time to PDFD was notably lower, at 0.1 octad for rainfed farmland. In the South China region, the average response time of NPP to HWFD was 0.3 octad for irrigated farmland and 1.1 octads for rainfed farmland. The response time to PDFD was 0.3 octad for irrigated and 0.6 for rainfed farmland. The Southwest region showed the average response time of NPP to HWFD at 1.4 octads for irrigated farmland and 2.0 octads for rainfed farmland. The response time to PDFD was 0.7 octad for irrigated and 0.6 octad for rainfed farmland. The average response time of NPP to HWFD was 1.2 octads for irrigated farmland and 1.0 octad for rainfed farmland in the YRML region. The response time to PDFD was 0.2 octad for irrigated farmland.

The response characteristics of NPP to different types of flash droughts vary across different types of farmlands (Fig. 7). The response frequency of NPP to HWFD peaked in May (33.3 % for irrigated farmland and 27.3 % for rainfed farmland). The response frequency of NPP to PDFD was highest in April (100 % for irrigated farmland and 52.9 % for rainfed farmland). Regarding different months, NPP exhibited higher response frequencies to flash droughts in April, May, and June and relatively lower response frequencies in July, August, and September.

NPP had the longest response time to HWFD in May (2.1 octads for irrigated farmland) and July (2.0 octads for rainfed farmland). The shortest response times for NPP to HWFD occurred in August (1.2 octads for irrigated farmland) and September (1 octad for rainfed farmland). The most extended response time for NPP to PDFD was in September (1.9 octads for irrigated farmland) and May (2.1 octads for rainfed farmland). The shortest response time for NPP to PDFD was in April (1 octad for irrigated farmland) and July (1 octad for rainfed farmland). March to May is the sowing period, during which the germinating crops have just begun to grow, and their root systems are not deep enough to access moisture from deeper soil layers, making them more susceptible to flash droughts.

In the GX region, NPP on farmland showed its highest response frequency to HWFD in May (46.7 % for irrigated farmland) and June (29.2 % for rainfed farmland) (Fig. S5). The peak response to PDFD occurred in June, with 29.5 % for irrigated farmland and 57.1 % for rainfed farmland. In the HHH region, the NPP response to HWFD was most pronounced in June, reaching 39.4 % for irrigated farmland and 22.9 % for rainfed farmland. For PDFD, the highest response frequency was also observed in June, with 61.7 % for irrigated farmland and 35.7 % for rainfed farmland. In the IMGW area, the NPP response to HWFD was most significant in May (100 % for rainfed farmland) and June (62.5 % for irrigated farmland). The response to PDFD consistently peaked in May and June at 100 % for irrigated and rainfed farmland. On the LP, the NPP response to HWFD was most frequent in May, with 22.2 % for irrigated farmland and 7.4 % for rainfed farmland. The response to PDFD peaked in June, with 21.1 % for irrigated farmland and 16.7 % for rainfed farmland. In the NE, the NPP response to HWFD was highest in May, at 100 % for irrigated farmland and 50 % for rainfed farmland. The response to PDFD was most notable in May (50 % for rainfed farmland) and June (100 % for rainfed farmland). In the QT region, the NPP response to HWFD was uniformly high in May, reaching 100 %. Similarly, the response to PDFD peaked in May, with a 100 % response frequency for rainfed farmland. In the South China region, the NPP response to HWFD was most significant in May, with 33.3 % for irrigated farmland and 55.3 % for rainfed farmland. The response to PDFD was consistently highest in April and June, reaching 100 %. In the SW region, the NPP response to HWFD was most pronounced in May and August, with 30 % for irrigated farmland and 42.9 % for rainfed farmland. The response to PDFD peaked in May and June, with 44.4 % for irrigated farmland and 50 % for rainfed farmland. In the YRML region, the NPP response to HWFD was most frequent in May and July, with 30 % for irrigated farmland and 32.5 % for rainfed farmland. The response to PDFD was highest in June, with 48 % for irrigated farmland.

The NPP of farmland responded most durably to HWFD in June for rainfed farmland (1.9 octads) and July for irrigated farmland (1.4 octads) in the GX region. The response to PDFD was most prolonged in May for irrigated farmland (3 octads) and June for rainfed farmland (1.1 octads). In the HHH region, NPP exhibited its most extended response times to HWFD in May, with 3 octads for irrigated farmland and 2.6 octads for rainfed farmland. The response to PDFD peaked in May at 2.1 octads for irrigated farmland and 2 octads for rainfed farmland. Along the IMGW area, NPP's most extended response times to HWFD were observed in June for irrigated farmland (1.1 octads) and May for rainfed farmland (1 octad). The response to PDFD was most sustained in May and June, lasting 1 octad for irrigated and rain-fed farmland. On the LP, the NPP's most enduring responses to HWFD were in July for rainfed farmland (4.5 octads) and August for irrigated farmland (2.7 octads). The response to PDFD was most extensive in June, with 1 octad for irrigated farmland and 2 octads for rainfed farmland. In the NE, the longest response time of NPP to HWFD was in June for rainfed farmland (1.2 octads) and July for irrigated farmland (1.5 octads). The response to PDFD was most prolonged in May and June, at 1 octad for rainfed and irrigated farmland. In the QT region, the most significant response time of NPP to HWFD was in May for rainfed farmland (14 octads) and September for irrigated farmland (3 octads). The response to PDFD was most extended in May, at 1 octad for rainfed farmland. In the South China region, the most enduring responses of NPP to HWFD were in July for irrigated farmland (1.3 octads) and August for irrigated farmland (2 octads). The response to PDFD was most sustained in April (1.8 octads for rainfed farmland) and June (1.5 octads for irrigated farmland). In the SW region, the longest response time of NPP to HWFD was in July, at 2.3 octads. The response to PDFD was most extended in May, with 3.5 octads for irrigated farmland and 3.2 octads for rainfed farmland. In the YRML region, NPP's most prolonged response time to HWFD was in May and June, with 1.4 octads for irrigated farmland and 1.5 octads for rainfed farmland. The longest response time to PDFD was in June, at 1.3 octads for irrigated farmland.

These observations indicated that most regions manifested their peak response frequencies to flash droughts during May and June. Regarding response duration, most regions exhibited relatively briefer periods in May and June, suggesting that farmland NPP was particularly sensitive to flash droughts at this time. This heightened sensitivity implies that crops are at a greater risk during these months. Consequently, crops are more vulnerable to threats during this period if a flash drought occurs.

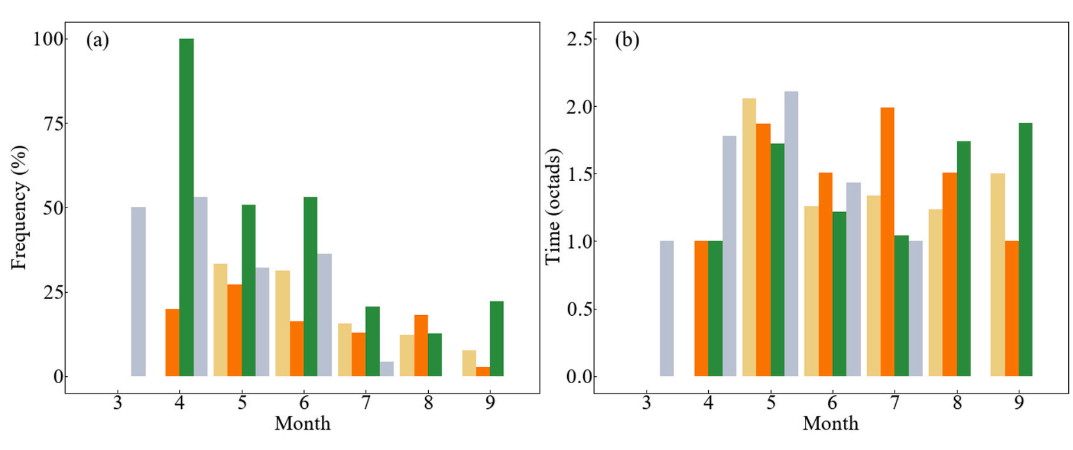

Fig. 7. Monthly variation in the response of NPP to flash droughts in different types of farmlands from 2000 to 2018.

Different regions' farmlands exhibited varied response characteristics to flash droughts (Fig. 8). In irrigated farmland, the HHH region's NPP showed the highest response frequency to flash droughts (28.8 % for HWFD and 59.7 % for PDFD). The NE's NPP in irrigated farmland had the lowest response frequency to HWFD, at 6.4 %; the LP's NPP in irrigated farmland had the lowest response frequency to PDFD, at 17.4 %. In rainfed farmland, South China's NPP had the highest response frequency to HWFD, at 39.4 %; the Gansu-Xinjiang region's NPP had the highest response frequency to PDFD, at 50 %. The LP's NPP in rainfed farmland had the lowest response frequency to flash droughts (5.7 % for HWFD and 11.5 % for PDFD).

In irrigated farmland, the LP's NPP had the longest response time to HWFD at 1.6 octads; the SW's NPP had the longest response time to PDFD at 3.5 octads. The NE's NPP in irrigated farmland had the shortest response time to flash droughts, both at 1 octad. In rainfed farmland, the LP's NPP had the longest response time to HWFD at 2.1 octads; the SW's NPP had the longest response time to PDFD at 3 octads. The NE's NPP in rainfed farmland had the shortest response time to flash droughts, both at 1.0 octad; the LP's NPP also had the shortest response time to PDFD, at 1.0 octad (Fig. 9b).

The NPP in irrigated farmland exhibited a higher response frequency to HWFD (24.37 %) and PDFD (37.88 %) than the NPP in rainfed farmland (21.75 % for HWFD and 29.76 % for PDFD), being 12 % and 27 % higher, respectively (Fig. 9). The NPP of rainfed farmland responded for a longer duration to HWFD (1.13 octads) and PDFD (0.83 octad) compared to the response time of NPP in irrigated farmland to flash droughts (0.89 octad for HWFD and 0.76 octad for PDFD), being 27 % and 9 % longer, respectively.

From both perspectives of response time and response frequency, it can be observed that the NPP of irrigated farmland was more sensitive to flash droughts (shorter response time and higher response frequency). Considering both flash droughts, NPP was more sensitive to PDFD (NPP responds with a shorter time and higher frequency to PDFD).

3.3. Resilience of NPP to flash drought

Fig. 10 illustrates changes in the NPP of different types of farmlands during different stages of flash droughts. In the GX region, after experiencing HWFD, there was a particular increase in NPP during the outbreak stage of the flash drought (except for PDFD-I). The NPP values during the recovery stage were higher than those during the accumulation stage (except for PDFD-I). This indicated that, aside from the weak resilience of irrigated farmland to PDFD, the resilience of farmland to HWFD and rainfed farmland to PDFD was quite strong.

In the HHH region, after experiencing HWFD, NPP increased to some extent during the outbreak stage, and the NPP values during the recovery stage were higher than those during the accumulation stage, indicating a strong resilience of NPP to HWFD in this region. For both types of farmland, NPP decreased to some extent during the outbreak stage of PDFD (compared to the accumulation stage), suggesting that the damage caused by PDFD to crops would be greater. The NPP values of irrigated farmland during the recovery stage were lower than those during the accumulation stage, indicating weak resilience of irrigated farmland to PDFD. In comparison, the NPP values of rainfed farmland during the recovery stage were higher than those during the accumulation stage, indicating strong resilience of rainfed farmland to PDFD.

In the IMGW, LP, and NE regions, the NPP values were higher during the outbreak and recovery stage than the accumulation stage, indicating strong resilience of farmlands to both types of flash droughts.

In the QT region, the NPP values of irrigated farmland were lower during the outbreak and recovery stages of HWFD than the accumulation stage, indicating weak resilience of irrigated farmland to HWFD. The NPP values of rainfed farmland were higher during the outbreak stage of both types of flash droughts compared to the accumulation stage, but they were lower during the recovery stage of HWFD and higher during the recovery stage of PDFD, indicating that rainfed farmland had a solid resilience to PDFD but a weak resilience to HWFD.

In the South China region, the NPP values were higher during the outbreak stage compared to the accumulation stage of both types of flash droughts, and the NPP values during the recovery stage of HWFD were higher than those during the accumulation stage, indicating strong resilience of farmland in the South China region to HWFD. However, the NPP values during the recovery stage of PDFD were lower than those during the accumulation stage, indicating the weak resilience of farmland in the South China region to PDFD.

In the SW region, the NPP values of irrigated farmland were higher during the outbreak and recovery stage of HWFD than the accumulation stage, indicating strong resilience of irrigated farmland to HWFD. The NPP of rainfed farmland in the SW region was lower during the recovery stage of HWFD than the accumulation stage, indicating weak resilience of rainfed farmland to HWFD. The NPP values of irrigated farmland in the SW region were lower during the outbreak and recovery stage of PDFD than the accumulation stage, indicating weak resilience of irrigated farmland to PDFD. The NPP values of rainfed farmland in the SW region were higher during the outbreak and recovery stages of PDFD than the accumulation stage, indicating strong resilience of rainfed farmland to PDFD.

In the YRML region, the NPP values of farmland were higher during the outbreak and recovery stage of HWFD compared to the accumulation stage, indicating strong resilience of farmland to HWFD. The NPP values of irrigated farmland in the YRML region were lower during the outbreak stage and higher during the recovery stage of PDFD compared

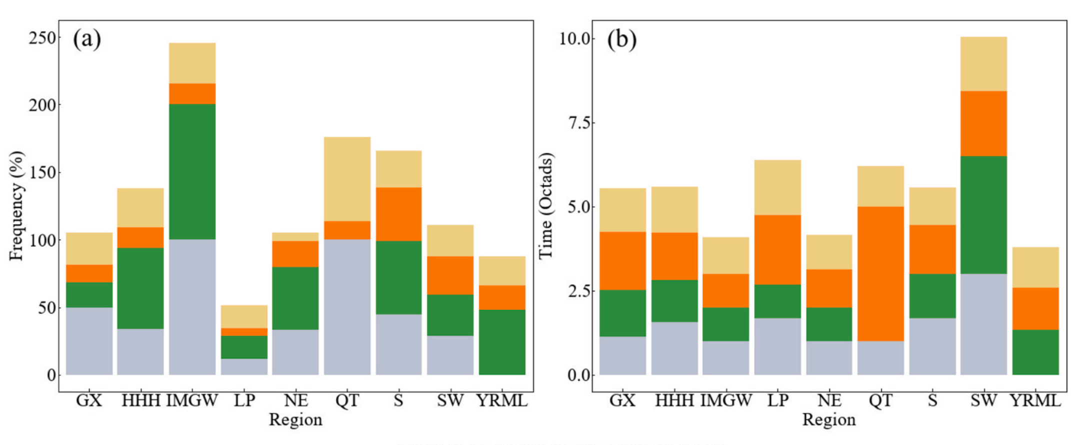

Fig. 8. Response of NPP in different types of farmlands to flash droughts across agricultural regions in China from 2000 to 2018. Note: Due to the limited number of grid points in the QT and IMGW, these areas are not considered in the comparison.

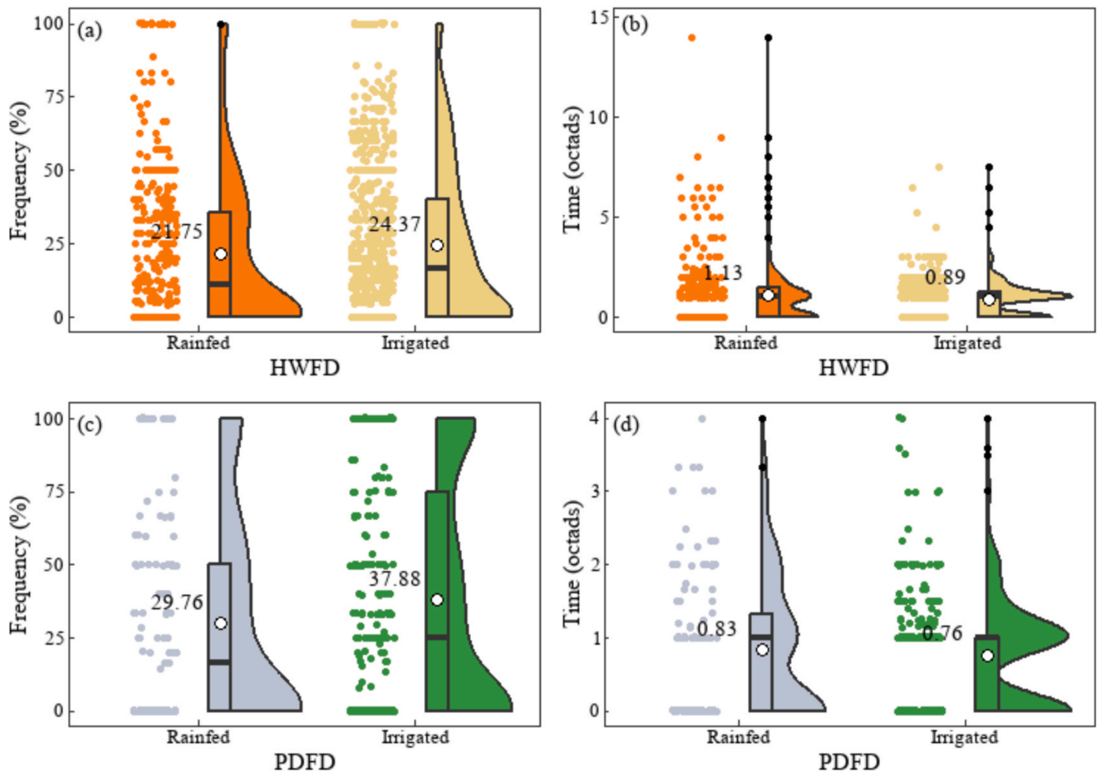

Fig. 9. Distribution map of NPP response to flash droughts in different types of farmlands in China from 2000 to 2018. Notes: The 0 in the figure represents grid points where no flash drought occurs.

to the accumulation stage, indicating strong resilience of irrigated farmland to PDFD. The NPP values of rainfed farmland in the YRML region were higher during the outbreak and recovery stages of PDFD than the accumulation stage, indicating the strong resilience of rainfed farmland to PDFD.

Different types of farmland in various regions exhibited varying resilience in response to flash droughts. Overall, the resilience of farmland to HWFD was relatively strong, while the resilience to PDFD was relatively weak. Rainfed farmland tended to have stronger resilience compared to irrigated farmland. The LP, NE, and YRML regions demonstrated strong resilience from flash droughts, with both types of farmland able to recover from both types of flash droughts.

4. Discussion

4.1. Impact of irrigation on the occurrence of flash droughts

This study found that the occurrence frequency and duration of HWFD in irrigated farmland were lower than in rainfed farmland. HWFD occurs due to high temperatures, increasing evapotranspiration, and reducing soil moisture (Mo and Lettenmaier, 2015). The most direct effect of irrigation is to replenish soil moisture, and an increase in soil moisture can raise the soil moisture quantiles during the irrigation period, reducing the likelihood of HWFD to some extent. Additionally, irrigation can lower temperatures (Cui et al., 2022; Mishra et al., 2020; Yang et al., 2020). Although the impact of irrigation on average temperatures is minimal, it can reduce the highest temperatures. This reduction in peak temperatures can shorten the periods that meet the conditions for the occurrence of HWFD, thereby reducing the frequency and duration of such events. Therefore, reducing temperature and increasing soil moisture due to irrigation can decrease the probability of HWFD. Numerous studies have indicated that changes in incremental soil moisture due to irrigation can lead to an increase in localized evapotranspiration and latent heat fluxes (Kang and Eltahir, 2018; Liu and Wang, 2023; Wang et al., 2021).

PDFD is caused by a lack of precipitation, leading to a reduction in ET, which causes an increase in temperature (Mo and Lettenmaier, 2016). Liu et al. (2021) found that the impact of irrigation on precipitation was mainly concentrated in the summer and autumn, with irrigation having a significant suppressive effect on precipitation in central and southwestern China. During these seasons, irrigation has a considerable impact on precipitation, which is primarily characterized by a decrease. The reduction in precipitation due to irrigation increases the likelihood of PDFD. At the same time, the increase in ET, temperature decrease, and soil moisture increase brought about by irrigation weaken the effects of PDFD. However, the mitigating effect of irrigation on PDFD was not as significant as one might expect (the occurrence frequency of PDFD in irrigated and rainfed farmland was not significantly different), possibly because the increase in ET caused by irrigation was not substantial enough to turn the negative anomalies of ET into positive ones.

4.2. Effects of irrigation on crop response

This study discovered that NPP in the HHH and S farmlands exhibited a high response frequency to flash droughts. Concurrently, Zhao et al. (2024) observed that the incidence of GPP displaying negative anomalies in tandem with flash droughts tended to impose a constraining impact on specific areas in Northwest and East China, whereas ecosystems in the Southwest and Northeast appear to be less impacted. The spatial distribution of the findings in this study aligns with those of Zhao et al. (2024), albeit with some numerical discrepancies. These discrepancies stem from using distinct indicators—NPP is calculated as the net result of GPP minus autotrophic respiration. The methodologies differ; the response frequency documented in this study is the ratio of instances where NPP manifests a negative anomaly after the outbreak of flash droughts relative to the total number of such events. The study's approach solely tallies the occurrences of NPP negative anomalies without specifying that these anomalies must coincide with the onset of

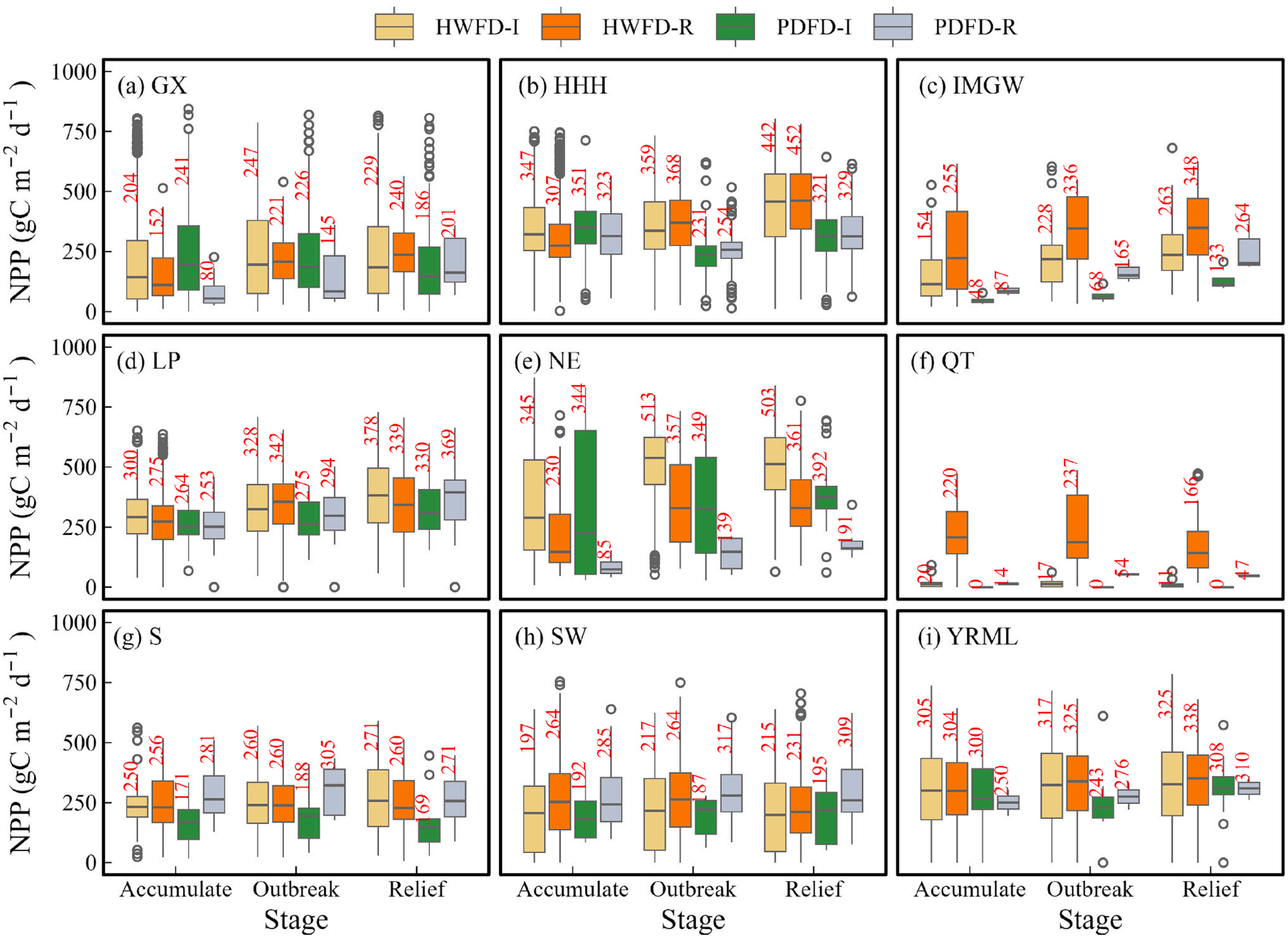

Fig. 10. Changes in NPP of different types of farmlands during different stages of flash droughts. The red text represents the average value of NPP. Due to the limited number of grid points in the QT and IMGW regions, these areas are not considered in comparison. (For interpretation of the references to colour in this figure legend, the reader is referred to the web version of this article.)

flash droughts.

Irrigation also impacts crops. At the leaf level, water affects the allocation of carbon and nitrogen between photosynthetic and non-photosynthetic tissues and controls the rates of photosynthesis and stomatal conductance (Ghannoum, 2008; Ozdogan, 2011). Irrigation increases moisture, which can enhance the intensity of photosynthesis and thereby increase NPP. Numerous studies have demonstrated that irrigation can increase NPP (Bradford et al., 2005; Li et al., 2022; Lobell et al., 2009; Zhuang et al., 2022). However, irrigation is not conducted year-round, meaning it can only increase NPP during specific periods, thereby endowing irrigated crops with some resistance to drought. Of course, the differences in the response characteristics of NPP to flash droughts between rainfed and irrigated crops may be related to the types of crops planted. Different crop types have varying root lengths, affecting their ability to extract water from deeper soil layers when faced with flash droughts, leading to different response characteristics.

This study found that irrigated crops had a higher response frequency and shorter response time to flash droughts, meaning that irrigated crops were more sensitive to flash droughts. Irrigated crops, which are long-term accustomed to moist conditions, struggle to adapt when drought occurs; hence, there is a greater sensitivity of NPP in irrigated farmland to flash droughts. The reduction in flash droughts due to changes in meteorological elements caused by irrigation may also lead to an increased response frequency in irrigated crops. If irrigation only prolongs the response time, and the decrease in flash droughts due to irrigation is more significant than the decrease in the number of responses, then the response frequency of crops to flash droughts also increases. The changes in latent heat flux, sensible heat flux, and transpiration caused by irrigation are also amplified due to the greening effect of irrigation (Liu and Wang, 2023). The impact of irrigation on meteorological variables and its influence on NPP are interactive. However, which element is more significantly affected by irrigation, leading to changes in response, remains unknown.

In addition, specific irrigation decisions in the face of drought also affect crop response to flash drought and the persistence of flash drought. Wang et al. (2018) conducted household surveys in 86 villages in five provinces, and they found that due to differences in the type of irrigation infrastructure accessed, some farmers increased irrigation in the face of drought while others did not. Farmers were more likely to increase irrigation in villages with high pond densities and better irrigation infrastructure in response to drought. There was also a positive correlation between the number of irrigations and the density of irrigation stations. If local communities have better irrigation infrastructure, farmers may have increased access to irrigation water, and their resilience to drought may be enhanced.

4.3. *Sensitivity and resilience of farmland NPP to flash droughts*

This study found that cultivated lands in the HHH and South China regions were relatively sensitive to flash droughts, with high response frequencies and short response times. This was partially consistent with the results of Zhang et al. (2020), which showed that NPP had shorter response times in North China. The differences in regional division between our study and theirs contributed to the discrepancies in results.

Zhang et al. (2020) divided the regions based on longitude and latitude, while this study used agricultural zoning. Different identification methods for flash droughts can also lead to varying results. This study found that NPP in all regions increased to some extent during flash droughts, consistent with Sun et al. (2016), who found that short-term droughts accompanied by high temperatures can increase NPP. The study revealed that the LP, NE, and YRML regions had strong resilience from flash droughts, and Kang and Zhang (2016) found that the Middle and Lower Yangtze River regions had good resistance to drought. Wang et al. (2022) pointed out that human activities have enhanced the drought resistance of the Loess Plateau. The construction of terraces and sediment dams in the Loess Plateau can reduce soil erosion and enhance crops' water and fertilizer retention capacity (Wei et al., 2016). Ridge furrow mulching transforms farmland into a micro-topography with alternating ridges and furrows, with the furrow surfaces wholly covered by mulch film, and crops are sown in the furrows (Zhao et al., 2014). Ridge furrow mulching cultivation can improve the water use efficiency of crops, collect precipitation and quickly infiltrate into the soil, reduce soil moisture evaporation, conserve natural precipitation, alleviate moisture stress caused by drought, and indirectly enhance the drought resistance of crops (Li et al., 2017). This study investigated the changes in crops during different periods of flash droughts; however, the impact of flash droughts occurring at different growth stages of crops is still unknown, and future research can be carried out in this direction.

4.4. Limitations and implications

This study also has certain limitations. First is the limitation brought by using a single reanalysis dataset. This paper only selected one dataset to identify flash droughts, possibly introducing inaccurate results. Secondly, our consideration is ideal, assuming that flash droughts cause all NPP anomalies. NPP is influenced by a variety of factors, such as the use of fertilizers, field management practices, floods, etc. (Herzog et al., 2019; Huang et al., 2024; Meng et al., 2024; Xia et al., 2023; Zhu et al., 2024). Other influencing factors beyond flash droughts must be excluded to assess crops' response to NPP accurately. Future research can eliminate these factors to accurately assess the response of crops to NPP. The NPP data used in this paper is an 8-day average, and the use of averages may cause the variation in data to disappear. Daily NPP values could be used to study crop responses if conditions allow. In addition, there are still some issues with the division of flash drought stages. Flash droughts can occur quickly, so defining the two octads before the flash drought as the accumulation period of flash drought may be too long or too short. Different vegetation has different sensitivities to flash droughts, so setting the recovery stage as one octad after the flash drought may not be reasonable. A negative value in crop NPP is considered a response to flash drought, but if this anomaly is too small, does the crop not respond to flash droughts? Should a threshold be set when studying crop responses? This paper studies the impact of flash droughts on crops during different periods of flash droughts, so it may also be possible to study the impact of flash droughts during different growth periods of crops.

5. Conclusions

With the identification of two types of flash droughts in China, HWFD occurred more frequently and had a longer duration than PDFD from 2000 to 2018. HWFD was more common in rainfed cropland, while PDFD tended to occur in irrigated cropland. The frequency of both flash droughts was highest in June, with higher frequency and duration in summer and lower in autumn. The frequency and duration of HWFD were high in the LP, while PDFD was relatively long in the GX and HHH regions, resulting in the LP, GX, and HHH disaster-prone areas. These findings have implications for disaster prevention and control in critical regions. HWFD was more frequent and lasted longer in rainfed cropland, whereas PDFD occurred more frequently and for longer durations in irrigated cropland, providing valuable insights for informed irrigation decisions.

The frequency and duration of flash droughts in China's cropland decreased from 2000 to 2018. Overall, the NPP response frequency to both flash drought types was low. NPP was more sensitive to PDFD regarding response frequency and response time (monthly and yearly variations). NPP in irrigated cropland was more sensitive to flash droughts, responding with high frequency in April, May, and June. The NPP of cropland in HHH and South China was more sensitive to flash drought, with high response frequency and relatively short response time. The resilience of different croplands to different types of flash droughts varied across regions. Croplands in each region were more resilient to HWFD and less resilient to PDFD. Rainfed cropland was more resilient to flash drought than irrigated cropland.

CRediT authorship contribution statement

Yuanxin Dai: Writing – review & editing, Writing – original draft, Visualization, Validation, Formal analysis. **Mengyuan Xu:** Writing – review & editing. **Jinlong Dong:** Software. **Ning Yao:** Methodology, Investigation, Funding acquisition, Conceptualization. **Yi Li:** Supervision. **Shibin Liu:** Writing – review & editing. **Tehseen Javed:** Writing – review & editing. **La Zhuo:** Writing – review & editing. **Qiang Yu:** Resources, Project administration.

Declaration of competing interest

The authors declare that they have no known competing financial interests or personal relationships that could have appeared to influence the work reported in this paper.

Acknowledgments

This research was partially supported by the National Natural Science Foundations of China (52209070 and U2243235), the Cyrus Tang Foundation Project, and the Shaanxi Provincial Water Conservancy Science and Technology Plan Project (2024slkj-10).

Appendix A. Supplementary data

Supplementary data to this article can be found online at https://doi.org/10.1016/j.ecolind.2025.113643.

Data availability

Data will be made available on request.

References

Bradford, J.B., Lauenroth, W.K., Burke, I.C., 2005. The impact of cropping on primary production in the US Great Plains. Ecology 86 (7), 1863–1872. https://doi.org/10.1890/04-0493.
Christian, J.I., et al., 2021. Global distribution, trends, and drivers of flash drought occurrence. Nat. Commun. 12 (1), 6330. https://doi.org/10.1038/s41467-021-26692-z.
Cui, F.Q., et al., 2022. Interplay Between Urbanization and Irrigation on Summer Climate in the Huang-Huai-Hai Plain, China. J. Geophys. Res.-Atmos. 127 (12). https://doi.org/10.1029/2021jd036053.
Defourny, P., et al., 2017. Land Cover Climate Change Initiative - Product User Guide v2. Issue 2.0.
FAO, 2003. Statistical databases.
Ford, T.W., Labosier, C.F., 2017. Meteorological conditions associated with the onset of flash drought in the eastern United States. Agric. For. Meteorol. 247, 414–423. https://doi.org/10.1016/j.agrformet.2017.08.031.
Gerken, T., Bromley, G.T., Ruddell, B.L., Williams, S., Stoy, P.C., 2018. Convective suppression before and during the United States Northern great plains flash drought of 2017. Hydrol. Earth Syst. Sci. 22, 4155–4163. https://doi.org/10.5194/hess-22-4155-2018.
Ghannoum, O., 2008. C4 photosynthesis and water stress. Ann. Bot. 103 (4), 635–644. https://doi.org/10.1093/aob/mcn093.

Griffin-Nolan, R.J., et al., 2019. Shifts in plant functional composition following long-term drought in grasslands. J. Ecol. 107 (5), 2133–2148. https://doi.org/10.1111/1365-2745.13252.
Herzog, C., et al., 2019. Crop yield, weed cover and ecosystem multifunctionality are not affected by the duration of organic management. Agr Ecosyst Environ 284, 106596. https://doi.org/10.1016/j.agee.2019.106596.
Huang, C.X., et al., 2024. Application of synthetic fertilizers with crop straw facilitates optimization of soil nematode community and supports crop yields. Appl. Soil Ecol. 197. https://doi.org/10.1016/j.apsoil.2024.105340.
Hunt, E., et al., 2021. Agricultural and food security impacts from the 2010 Russia flash drought. Weather Clim. Extremes 34, 100383. https://doi.org/10.1016/j.wace.2021.100383.
Jiang, Z., et al., 2019. Future changes in rice yields over the Mekong River Delta due to climate change-Alarming or alerting? Theor. Appl. Climatol. 137 (1), 545–555. https://doi.org/10.1007/s00704-018-2617-z.
Jin, C., Luo, X., Xiao, X., Dong, J., Li, X., Yang, J., Zhao, D., 2019. The 2012 flash drought threatened US Midwest agroecosystems[J]. Chin. Geogr. Sci. 29, 768–783.
Kang, L., Zhang, H., 2016. A Comprehensive Study of Agricultural Drought Resistance and Background Drought Levels in Five Main Grain-Producing Regions of China. Sustainability 8 (4), 346.
Kang, S., Eltahir, E.A.B., 2018. North China Plain threatened by deadly heatwaves due to climate change and irrigation. Nat. Commun. 9. https://doi.org/10.1038/s41467-018-05252-y.
Li, C.J., et al., 2017. Ridge-furrow with plastic film mulching practice improves maize productivity and resource use efficiency under the wheat-maize double-cropping system in dry semi-humid areas. Field Crop Res 203, 201–211. https://doi.org/10.1016/j.fcr.2016.12.029.
Li, T.C., et al., 2022. Carbon Budget of Paddy Fields after Implementing Water-Saving Irrigation in Northeast China. Agronomy-Basel 12 (6). https://doi.org/10.3390/agronomy12061481.
Liu, G.S., Wang, W.G., 2023. Irrigation-Induced Crop Growth Enhances Irrigation Cooling Effect Over the North China Plain by Increasing Transpiration. Water Resour. Res. 59 (3). https://doi.org/10.1029/2022wr034142.
Liu, J., Jin, J.M., Niu, G.Y., 2021. Effects of Irrigation on Seasonal and Annual Temperature and Precipitation over China Simulated by the WRF Model. J. Geophys. Res.-Atmos. 126 (10). https://doi.org/10.1029/2020JD034222.
Liu, X., Liu, X., Yang, Y., Yu, M., Tian, H., 2024. The productivity anomalies and economic losses of different grassland ecosystems caused by flash drought. Agric Water Manag 305, 109139. https://doi.org/10.1016/j.agwat.2024.109139.
Liu, X.X., Liu, X.M., Yu, M., Zhao, H.Y., Zhu, Z.Y., 2024. Productivity response characteristics of different grasslands to flash drought and their relationship with drought tolerance. Ecol. Ind. 159. https://doi.org/10.1016/j.ecolind.2024.111761.
Liu, Y., et al., 2020. Flash droughts characterization over China: From a perspective of the rapid intensification rate. Sci. Total Environ. 704, 135373. https://doi.org/10.1016/j.scitotenv.2019.135373.
Lobell, D.B., Cassman, K.G., Field, C.B., 2009. Crop yield gaps: their importance, magnitudes, and causes. Annu. Rev. Env. Resour. 34, 179–204. https://doi.org/10.1146/annurev.environ.041008.093740.
Lovino, M.A., et al., 2025. Agricultural flash droughts and their impact on crop yields in southeastern South America. Environ. Res. Letters.https://doi.org/10.1088/1748-9326/adcd88.
Lu, M.G., et al., 2024. Heterogeneity in vegetation recovery rates post-flash droughts across different ecosystems. Environ. Res. Lett. 19 (7). https://doi.org/10.1088/1748-9326/ad5570.
Mahto, S.S., Mishra, V., 2023. Increasing risk of simultaneous occurrence of flash drought in major global croplands. Environ. Res. Lett. 18 (4). https://doi.org/10.1088/1748-9326/acc8ed.
Meng, H.Y., Qian, L., Duan, K., 2024. Evaluating the impacts of flooding on crop yields by different meteorological indices: A regional case study in the middle-lower reach of the Yangtze River. China. Ecological Indicators 162. https://doi.org/10.1016/j.ecolind.2024.112068.
Mishra, V., et al., 2020. Moist heat stress extremes in India enhanced by irrigation. Nat. Geosci. 13 (11), 722-+. https://doi.org/10.1038/s41561-020-00650-8.
Mo, K.C., Lettenmaier, D.P., 2015. Heat wave flash droughts in decline. Geophys. Res. Lett. 42 (8), 2823–2829. https://doi.org/10.1002/2015GL064018.
Mo, K.C., Lettenmaier, D.P., 2016. Precipitation deficit flash droughts over the United States. J. Hydrometeorol. 17 (4), 1169–1184. https://doi.org/10.1175/JHM-D-15-0158.1.
Niu, J., Chen, J., Sun, L., Sivakumar, B., 2018. Time-lag effects of vegetation responses to soil moisture evolution: a case study in the Xijiang basin in South China. Stoch. Env. Res. Risk A. 32, 2423–2432. https://doi.org/10.1007/s00477-017-1492-y.
Otkin, J.A., et al., 2016. Assessing the evolution of soil moisture and vegetation conditions during the 2012 United States flash drought. Agric. For. Meteorol. 218, 230–242. https://doi.org/10.1016/j.agrformet.2015.12.065.
Otkin, J.A., Svoboda, M., Hunt, E.D., Ford, T.W., Anderson, M.C., Hain, C., Basara, J.B., 2018. Flash droughts: A review and assessment of the challenges imposed by rapid-onset droughts in the United States[J]. Bull. Amer. Meteor. Soc. 99 (5), 911–919.
Ozdogan, M., 2011. Exploring the potential contribution of irrigation to global agricultural primary productivity. Global Biogeochem. Cycles 25. https://doi.org/10.1029/2009gb003720.
Poonia, V., Goyal, M.K., Jha, S., Dubey, S., 2022. Terrestrial ecosystem response to flash droughts over India. J. Hydrol. 605. https://doi.org/10.1016/j.jhydrol.2021.127402.
Ren, T., Li, S., Duan, K., He, J., 2023. Spatiotemporal variation characteristics and influencing factors of heat wave and precipitation deficit flash drought in the Loess Plateau. Arid Land Geography 46 (03), 360–370. https://doi.org/10.12118/j.issn.1000-6060.2022.307.
Stocker, B.D., et al., 2018. Quantifying soil moisture impacts on light use efficiency across biomes. New Phytol. 218 (4), 1430–1449. https://doi.org/10.1111/nph.15123.
Sun, B.F., Zhao, H., Wang, X.K., 2016. Effects of drought on net primary productivity: Roles of temperature, drought intensity, and duration. Chin. Geogr. Sci. 26 (2), 270–282. https://doi.org/10.1007/s11769-016-0804-3.
Sun, R. et al., 2020. Global vegetation productivity from 1981 to 2018 estimated from remote sensing data.
Sungmin, O., Park, S.K., 2023. Flash drought drives rapid vegetation stress in arid regions in Europe. Environ. Res. Lett. 18 (1). https://doi.org/10.1088/1748-9326/acae3a.
Troy, T.J., Kipgen, C., Pal, I., 2015. The impact of climate extremes and irrigation on US crop yields. Environ. Res. Lett. 10 (5). https://doi.org/10.1088/1748-9326/10/5/054013.
Tyagi, S., et al., 2022. Flash Drought: Review of Concept, Prediction and the Potential for Machine Learning. Deep Learning Methods. EARTHS FUTURE 10 (11). https://doi.org/10.1029/2022EF002723.
Wang, D., et al., 2022. Drought Resistance of Vegetation and Its Change Characteristics before and after the Implementation of the Grain for Green Program on the Loess Plateau. China. Remote Sensing 14 (20), 5142.
Wang, W.G., et al., 2021. The climatic effects of irrigation over the middle and lower reaches of the Yangtze River. China. Agricultural and Forest Meteorology 308. https://doi.org/10.1016/j.agrformet.2021.108550.
Wang, Y.J., Huang, J.K., Wang, J.X., Findlay, C., 2018. Mitigating rice production risks from drought through improving irrigation infrastructure and management in China. Aust. J. Agric. Resour. Econ. 62 (1), 161–176. https://doi.org/10.1111/1467-8489.12241.
Wei, W., et al., 2016. Global synthesis of the classifications, distributions, benefits and issues of terracing. Earth Sci. Rev. 159, 388–403. https://doi.org/10.1016/j.earscirev.2016.06.010.
Xia, H.Y., et al., 2023. Dissecting the relationship between yield and mineral nutriome of wheat grains in double cropping as affected by preceding crops and nitrogen application. Field Crop Res 293. https://doi.org/10.1016/j.fcr.2023.108845.
Xiao, M., Zhang, Q., Singh, V.P., Chen, X., 2013. Regionalization-based spatiotemporal variations of precipitation regimes across China. Theor. Appl. Climatol. 114, 203–212. https://doi.org/10.1007/s00704-013-0832-1.
Xu, H., Wang, X., Zhao, C., 2021. Drought sensitivity of vegetation photosynthesis along the aridity gradient in northern China. Int. J. Appl. Earth Obs. Geoinf. 102, 102418. https://doi.org/10.1016/j.jag.2021.102418.
Yang, L.Y., Wang, W.G., Wei, J., 2023. Assessing the response of vegetation photosynthesis to flash drought events based on a new identification framework. Agric. For. Meteorol. 339. https://doi.org/10.1016/j.agrformet.2023.109545.
Yang, Q.Q., Huang, X., Tang, Q.H., 2020. Irrigation cooling effect on land surface temperature across China based on satellite observations. Sci. Total Environ. 705. https://doi.org/10.1016/j.scitotenv.2019.135984.
Yao, T.T., Liu, S.X., Hu, S., Mo, X.G., 2022. Response of vegetation ecosystems to flash drought with solar-induced chlorophyll fluorescence over the Hai River Basin, China during 2001-2019. J. Environ. Manage. 313. https://doi.org/10.1016/j.jenvman.2022.114947.
Yuan, X., Ma, Z., Pan, M., Shi, C., 2015. Microwave remote sensing of short-term droughts during crop growing seasons. Geophys. Res. Lett. 42 (11), 4394–4401. https://doi.org/10.1002/2015GL064125.
Yuan, X., Wang, L., Wood, E.F., 2018. Anthropogenic intensification of southern African flash droughts as exemplified by the 2015/16 season. Bull. Am. Meteorol. Soc. 99 (1), S86–S90. https://doi.org/10.1175/BAMS-D-17-0077.1.
Yuan, X., et al., 2019. Anthropogenic shift towards higher risk of flash drought over China. Nat. Commun. 10 (1), 4661. https://doi.org/10.1038/s41467-019-12692-7.
Yuan, X., et al., 2023. A global transition to flash droughts under climate change. Science 380 (6641), 187–191. https://doi.org/10.1126/science.abn6301.
Zhang, M., Yuan, X., Otkin, J.A., 2020. Remote sensing of the impact of flash drought events on terrestrial carbon dynamics over China. Carbon Balance Manag. 15 (1). https://doi.org/10.1186/s13021-020-00156-1.
Zhang, M., et al., 2025. A pronounced decline in northern vegetation resistance to flash droughts from 2001 to 2022. Nat. Commun. 16 (1), 2984. https://doi.org/10.1038/s41467-025-58253-z.
Zhang, Y., et al., 2022. A new multi-variable integrated framework for identifying flash drought in the Loess Plateau and Qinling Mountains regions of China. Agric Water Manag 265, 107544. https://doi.org/10.1016/j.agwat.2022.107544.
Zhang, Y., Liu, F., Liu, T., Chen, C., Lu, Z., 2024. Characteristics of Vegetation Photosynthesis under Flash Droughts in the Major Agricultural Areas of Southern China. Atmos. 15 (8), 886. https://doi.org/10.3390/atmos15080886.
Zhu, Y., et al., 2025. Differential impact of flash droughts on water use efficiency in terrestrial ecosystems in Central Asia. Clim. Change 178 (3), 53. https://doi.org/10.1007/s10584-025-03894-8.
Zhao, H., et al., 2014. Ridge-furrow with full plastic film mulching improves water use efficiency and tuber yields of potato in a semiarid rainfed ecosystem. Field Crop Res 161, 137–148. https://doi.org/10.1016/j.fcr.2014.02.013.
Zhao, Y., et al., 2024. Understanding the effects of flash drought on vegetation photosynthesis and potential drivers over China. Sci. Total Environ. 931, 172926. https://doi.org/10.1016/j.scitotenv.2024.172926.

Zhu, L., et al., 2024. Optimizing crop yields while minimizing environmental impact through deep placement of nitrogen fertilizer. J. Integr. Agric. https://doi.org/10.1016/j.jia.2024.05.012.
Zhu, X.F., Liu, Y., Xu, K., Pan, Y.Z., 2021. Effects of Drought on Vegetation Productivity of Farmland Ecosystems in the Drylands of Northern China. Remote Sens. (Basel) 13 (6). https://doi.org/10.3390/rs13061179.
Zhuang, Q.W., et al., 2022. Unequal weakening of urbanization and soil salinization on vegetation production capacity. Geoderma 411. https://doi.org/10.1016/j.geoderma.2022.115712.

Further reading

Zhang, M., Yuan, X., 2020. Rapid reduction in ecosystem productivity caused by flash droughts based on decade-long FLUXNET observations. Hydrol. Earth Syst. Sci. 24 (11), 5579–5593. https://doi.org/10.5194/hess-24-5579-2020.